



A Single Natural Variation Determines Cytosolic Ca^{2+} -Mediated Hyperthermosensitivity of TRPA1s from Rattlesnakes and Boas

Eun Jo Du and KyeongJin Kang*

Department of Anatomy and Cell Biology and Samsung Biomedical Research Institute, Samsung Medical Center, Sungkyunkwan University School of Medicine, Suwon 16419, Korea

*Correspondence: kangk@skku.edu

<https://doi.org/10.14348/molcells.2020.0036>

www.molcells.org

Transient receptor potential ankyrin 1 from rattlesnakes (rsTRPA1) and boas (bTRPA1) was previously proposed to underlie thermo-sensitive infrared sensing based on transcript enrichment in infrared-sensing neurons and hyper-thermosensitivity expressed in *Xenopus* oocytes. It is unknown how these TRPA1s show thermosensitivities that overwhelm other thermoreceptors, and why rsTRPA1 is more thermosensitive than bTRPA1. Here, we show that snake TRPA1s differentially require Ca^{2+} for hyper-thermosensitivity and that predisposition to cytosolic Ca^{2+} potentiation correlates with superior thermosensitivity. Extracellularly applied Ca^{2+} upshifted the temperature coefficients (Q10s) of both TRPA1s, for which rsTRPA1, but not bTRPA1, requires cytosolic Ca^{2+} . Intracellular Ca^{2+} chelation and substitutive mutations of the conserved cytosolic Ca^{2+} -binding domain lowered rsTRPA1 thermosensitivity comparable to that of bTRPA1. Thapsigargin-evoked Ca^{2+} or calmodulin little affected rsTRPA1 activity or thermosensitivity, implying the importance of precise spatiotemporal action of Ca^{2+} . Remarkably, a single rattlesnake-mimicking substitution in the conserved but presumably dormant cytosolic Ca^{2+} -binding domain of bTRPA1 substantially enhanced thermosensitivity through cytosolic Ca^{2+} like rsTRPA1, indicating the capability of this single site in the determination of both cytosolic Ca^{2+} dependence and thermosensitivity. Collectively, these data suggest that Ca^{2+} is essential for the hyper-thermosensitivity

of these TRPA1s, and cytosolic potentiation by permeating Ca^{2+} may contribute to the natural variation of infrared senses between rattlesnakes and boas.

Keywords: Ca^{2+} binding, nonsynonymous substitution, pit vipers, Q10 scanning, snake infrared sense, TRPA1

INTRODUCTION

The ability of snakes to sense infrared radiation is mediated by facial sensory organs such as the rattlesnake pit organ located between the eye and the nostril, which harbors the infrared-receiving pit membrane densely innervated by trigeminal nerve endings (Bakken and Krochmal, 2007; Bullock and Fox, 1957). By contrast, the pit organs of the boa have a simpler design with or without shallow depression in the labial scales (Noble and Schmidt, 1937; Warren and Proske, 1968). Transient receptor potential ankyrin 1 (TRPA1) has been attributed to the molecular basis of infrared sensing observed in pit-bearing snakes, as its transcripts were heavily expressed compared with other genes in trigeminal neurons but not in dorsal root ganglia, only when the snakes are associated with an infrared-sensing capacity (Gracheva et al., 2010). Heterologously expressed rattlesnake and boa TRPA1s (rs- and bTRPA1s, respectively) were activated by increases

Received 2 February, 2020; revised 21 March, 2020; accepted 11 May, 2020; published online 2 June, 2020

eISSN: 0219-1032

©The Korean Society for Molecular and Cellular Biology. All rights reserved.

©This is an open-access article distributed under the terms of the Creative Commons Attribution-NonCommercial-ShareAlike 3.0 Unported License. To view a copy of this license, visit <http://creativecommons.org/licenses/by-nc-sa/3.0/>.

in temperature, supporting the thermosensitive hypothesis that temperature increases in the pit membrane by infrared irradiation stimulate thermosensitive neurons for infrared imaging in the brain. The photochemical hypothesis, in which photochemical reactions enable detection of infrared radiation as found with visible light utilizing photoisomerization of opsin-bound 11-cis-retinal, was further ruled out by a subsequent study showing that temperature coefficients (Q10s) of rsTRPA1 and bTRPA1 reach as high as ~100,000 and ~3,000, respectively, when heterologously assessed in *Xenopus* oocytes (Kang, 2016a). Q10 is a popular measure of ion channel thermosensitivity defined to represent a fold current increase by a temperature increase of 10°C (Kang, 2016a; Kang et al., 2012; Liu et al., 2003). Typical ion channels unrelated to thermal sensation show Q10s between 1 and 3. Interestingly, the heterologous study also found that Q10s of snake TRPA1s were higher when the amplitudes of thermally evoked currents were large. This positive Q10/amplitude relationship was much more evident in rsTRPA1 than bTRPA1. For large rsTRPA1 currents, the thermosensitivity/amplitude relationship was dramatically shifted from a slope of 473 to 6,725 (Q10/ μ A). In contrast, the slope of the thermosensitivity/amplitude relationship obtained from bTRPA1 was low (Q10 of 64/ μ A) compared with that of rsTRPA1 and remained monotonous throughout a wide range of current amplitudes, implying that activity-dependent regulation of rsTRPA1 is more complex and impactful than that of bTRPA1. Such thermosensitivities/amplitude relationships different between the two snake TRPA1s were coherently seen by means of various analyses such as Q10 scanning, Arrhenius plots (Kang, 2016a; Liu et al., 2003), Boltzmann slope factors, and the molar heat capacity changes (Clapham and Miller, 2011; Kang, 2016b). Thus, previous analyses on the snake TRPA1s suggest that the differential abilities of infrared detection between rattlesnakes and boas (Campbell et al., 2002; de Cock Buning, 1983) may be attributed to the difference in thermosensitivity of TRPA1 (Kang, 2016a; 2016b) in addition to their anatomical differences described above. Despite this, it remains unknown why the two TRPA1 channels show such distinct thermal responses.

A hypothesis was previously proposed to address this unique observation on these snake TRPA1s (Kang, 2016a). The cation influx through the channel may potentiate thermal rsTRPA1 activation, leading to a high Q10/amplitude relationship. Consistent with this view, we here show that rsTRPA1 and bTRPA1 require extracellular Ca²⁺ to enhance their thermosensitivities. In particular, extracellularly applied Ca²⁺ appears to be necessary to flow in to the cytosol for robust thermal sensitivity of rsTRPA1 but not that of bTRPA1. Given that TRPA1s are generally known to conduct cations in a non-selective manner, we provide several lines of experimental evidence to elucidate that Ca²⁺ influx through rsTRPA1 leads to potentiation of thermosensitivity through cytosolic Ca²⁺. Therefore, Ca²⁺ elevates thermal sensitivities of snake TRPA1s, further promoting the thermosensitive hypothesis of snake infrared sensing, and our data illustrating TRPA1 potentiation by permeating Ca²⁺ address how rattlesnakes are equipped with a much more sensitive ability of infrared detection than boas at the molecular level of thermoreceptors.

MATERIALS AND METHODS

Chemicals

EDTA (ED1041) and CaCl₂ (CC1080) were purchased from GeorgiaChem (USA). Sigma-Aldrich (USA) supplied BaCl₂ (202738), thapsigargin (T9033), BAPTA (14513), EGTA (E3889), and other essential chemicals.

Two-electrode voltage clamping on *Xenopus* oocytes

Thermally evoked current recordings in *Xenopus laevis* oocytes were acquired as described with minor modifications (Kang et al., 2010; 2012). Briefly, ovaries were surgically obtained from oocyte-positive *X. laevis* females commercially available from the Korean *Xenopus* Resource Center for Research in Korea (<https://www.aris.re.kr/app/main/mainView.do>). The ovaries were then placed under collagenase treatment at 1.5 mg/ml of collagenase type II (Worthington, USA) for 90 min with gentle rocking. Capped RNA (cRNA) was prepared by *in vitro* transcription with the use of mMessage mMachine T7 kit (Ambion, USA) to express snake TRPA1s (pMO rsTRPA1 and pMO bTRPA1 plasmids [Gracheva et al., 2010], gifts from Dr. David Julius at UCSF). *Drosophila* TRPA1 (TRPA1(B)) has been described in our recent studies (Du et al., 2016a; 2016b; 2019; Hamada et al., 2008; Kang, 2016a; Kang et al., 2010; 2012). Before *in vitro* transcription, the plasmids of snake TRPA1s were linearized with HpaI, and that of dTRPA1 was with SacI for run-off transcription termination. Following injection of 50 nl of *TrpA1* cRNA, oocytes were incubated for one day at 18°C in the Barth's solution (100 NaCl, 1 KCl, 1 MgCl₂, 0.5 CaCl₂, 0.33 Ca(NO₃)₂, 5 HEPES, pH 7.6 in mM). For temperature-evoked current recordings, cells were perfused in the recording solution (100 NaCl, 1 KCl, 1 MgCl₂, 5 HEPES, pH 7.6, 0.01 MONNA, and 0.01 flufenamic acid in mM), which was varied to provide different divalent cation conditions by including either 0.25 mM EDTA, 0.1 or 0.8 mM CaCl₂, or 2 mM BaCl₂. Typically, oocytes exhibited resting membrane potentials below -10 mV in these buffers and were analyzed only when the leak current at the beginning is below 500 nA. Voltage was initially held at -60 mV and ramped to +60 mV for 300 ms every second. The current was registered at 2,000 Hz by the GeneClamp 500B amplifier (Molecular Devices, USA) and subjected to data acquisition (Digidata 1440A; Molecular Devices). Temperature of the perfusion buffer was controlled to rise at ~0.5°C/s by SC-20 in-line heater/cooler (Warner Instruments, USA) with a CL100 biopolar temperature controller (Warner Instruments). Handling of the oocytes-donating frogs was conducted in accordance with the guideline which was approved by the Institutional Animal Care and Use Committee at Sungkyunkwan University in Korea (SKKUI-ACUC-20140036).

Q10 scanning

Q10 scanning was performed as established previously (Kang, 2016a) with minor modification. From the current recorded with voltage ramps, the current points at -60 mV were extracted using Clampfit 10.3 and transferred to Microsoft Excel. In this way, noise reduction or data smoothing processes could be omitted unlike the previous report (Kang,

2016a). In turn, Q10 was calculated by its definition $Q10 = (I_2 / I_1)^{10/(t_2-t_1)}$ with the use of two current and temperature data points apart from each other by 5 s corresponding to 2.5°C. The series of calculated Q10 at 1 Hz was plotted as function of the temperature t_1 .

Site-directed mutagenesis

Mutagenesis was performed as described previously (Kang et al., 2005a; 2005b). Substitutions in TRPA1s were made by swapping a region of wild-type (WT) cDNA sequence with a mutated cassette. A pair of mutually complementary oligonucleotide primers with a desired mutation were purchased, and each of them was paired with either upstream or downstream primers for the first two polymerase chain reaction (PCR) fragments, which overlap in the mutant primer-annealing region that contains the replaced codons, and served as template for the second PCR reaction amplified only with the upstream and downstream primers. The upstream and downstream primers were 40 base pairs away from unique restriction endonuclease target sites used to clone the second PCR products back in the WT cDNA background sequence. The 40 bp space between upstream and downstream primers and the restriction sites permits utilization of the primers for nucleotide sequencing reactions reading through the restriction site sequences. The fragments amplified by PCR were confirmed by sequencing after cloning to make sure that only desired mutations were introduced in the final cDNA constructs.

Statistical analysis

Statistical analyses were performed with Sigmaplot14.0 (SYSTAT Software, USA). For parametric tests, normality and homoscedasticity were examined by Shapiro–Wilk and Brown–Forsythe tests, respectively. When normality and equal variance were established, unpaired *t*-tests (two-sided) or ANOVA/Tukey post-hoc tests were performed. When normality or homoscedasticity tests failed, rank tests were used; Mann–Whitney U tests and Kruskal–Wallis one-way ANOVA with Dunn's tests were performed. Unless otherwise indicated, *, **, and *** are $P < 0.05$, 0.01, and 0.001 for parametric tests, respectively, and #, ##, and ### represent $P < 0.05$, 0.01, and 0.001, respectively, for nonparametric tests. In some instances, letters were used to indicate statistical differences between groups: a, b, c... for parametric tests and p, q, r... for nonparametric tests.

RESULTS

To examine whether thermal activation of TRPA1s can be modulated by extracellular Ca²⁺, *Xenopus* oocytes expressing TRPA1s were subjected to two-electrode voltage clamping, during which time the temperature of the perfusion buffer was increased by approximately 0.5°C/s (Figs. 1A–1I, upper and middle panels). Q10 was extracted from the current/temperature recordings with the use of the Q10 scanning method (Figs. 1A–1I, bottom panels) established in our previous studies (Kang, 2016a; 2016b). Similar to Q10 acquisition by the Arrhenius analysis (Kang, 2016a; Liu et al., 2003), Q10 scanning yields a value representing the highest thermosen-

sitivity point called peak Q10 (Q10p) (Figs. 1A–1J). As Q10s were acquired by exponential calculations (see Materials and Methods section), the data were log-transformed to attempt to achieve normal distribution and subsequently analyzed and plotted. When Ca²⁺-chelated (containing 0.25 mM EDTA) extracellular recording solution (100 mM NaCl, 1 mM KCl, 1 mM MgCl₂, 5 mM HEPES, pH 7.6) was perfused, rsTRPA1 and bTRPA1 showed mean logQ10ps ± SEM of 3.53 ± 0.14 (Q10 of 3,388.4) and 1.85 ± 0.11 (Q10 of 70.8), respectively. Interestingly, addition of 0.1 mM Ca²⁺ in the recording buffer (without EDTA) dramatically increased their logQ10ps to 4.60 ± 0.21 (Q10 of 39,810.7) and 2.44 ± 0.10 (Q10 of 275.4), respectively (Fig. 1J), while current amplitudes were comparable between experimental groups (Fig. 1L). The thermosensitivity of rsTRPA1 but not bTRPA1 was also stimulated to reach mean logQ10p ± SEM of 4.86 ± 0.10 (Q10 of 72,443.6) by 2 mM Ba²⁺ in the perfusion solution, suggesting distinct characteristics of the putative cation-binding pockets of the two TRPA1s. In contrast, indicative of snake-specific Q10 potentiation by Ca²⁺, Q10p of the thermosensitive *Drosophila* TRPA1(B) isoform (dTRPA1) (8) was little shifted by the additional divalent cations. The temperature point producing Q10p was denoted as the peak temperature (Tp) (Fig. 1K) to compare temperatures at which the channels exhibit robust thermal sensitivity. Addition of either Ca²⁺ or Ba²⁺ slightly yet significantly lowered the Tp of rsTRPA1, but not those of the other two TRPA1s. Note that the endogenous Ca²⁺-activated chloride current (CaCC) was suppressed by a combination of potent *Xenopus* anoctamin 1 inhibitors, N-((4-methoxy)-2-naphthyl)-5-nitroanthranilic acid (MONNA) (Oh et al., 2013) and flufenamate (Guinamard et al., 2013), and that contamination of much less temperature-sensitive currents like CaCC in the tested temperature range lead to underestimation of Q10 caused by larger fractional increase of the current denominator in exponential Q10 calculation. In addition, CaCC in *X. laevis* oocytes is not provoked by Ba²⁺ (Oh et al., 2008). After a temperature drop from the highest point on the temperature ramp to room temperature, cells perfused with 2 mM Ba²⁺ often left relatively large residual currents of rsTRPA1 with increased time constants of the slow deactivation component (Fig. 1C, Supplementary Fig. S1A), indicating that Ba²⁺ interferes with cooling-induced fast deactivation of rsTRPA1.

As TRPA1s are non-selective cation channels that readily conduct Ca²⁺, mammalian TRPA1s have been reported to be under modulation by permeating Ca²⁺ (Hasan et al., 2017; Wang et al., 2008; Zurborg et al., 2007). To test this possibility, oocytes expressing Ca²⁺-modulated TRPA1, rsTRPA1, or bTRPA1, were microinjected with chelators, while the normal Barth's solution containing 0.8 mM Ca²⁺ was used for perfusion. Injection of either 1,2-bis(o-aminophenoxy) ethane-N,N,N',N'-tetraacetic acid (BAPTA) or ethylene glycol-bis(β-aminoethyl ether)-N,N,N',N'-tetraacetic acid (EGTA) to a final concentration of 1 mM or 2.5 mM, respectively, resulted in dramatic decreases of Q10p in rsTRPA1-expressing cells (Figs. 2A–2C, Supplementary Fig. S1B). Consistent with the faster chelation kinetics of BAPTA than EGTA (You et al., 1997), BAPTA-injected rsTRPA1 cells showed a severe drop from 0.8 mM-Ca²⁺-evoked logQ10p of 5.79 ± 0.30

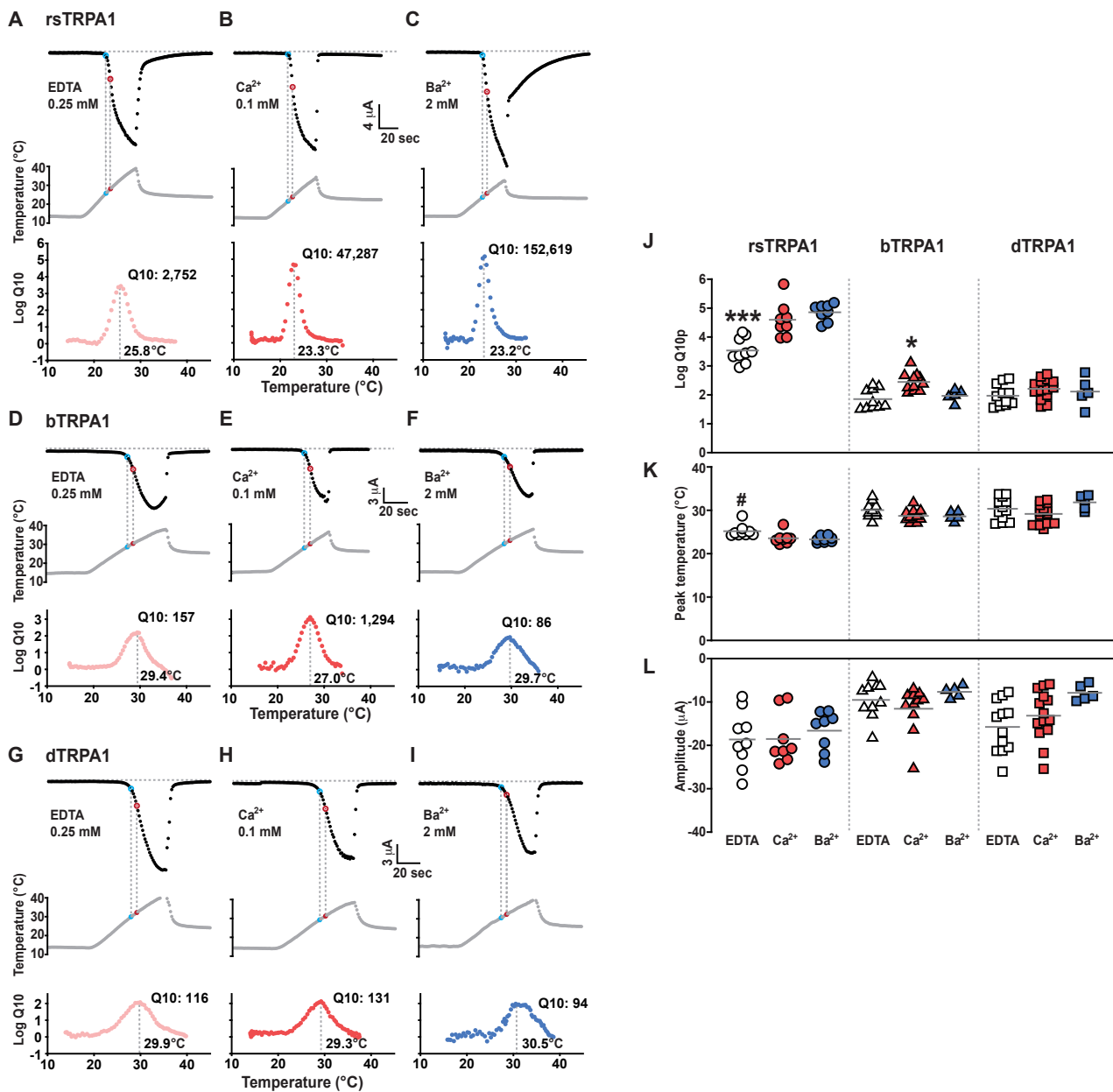


Fig. 1. Extracellularly applied divalent cations increase thermosensitivities of TRPA1s from infrared-sensing snakes. (A-I) Representative temperature-dependent current recordings and Q10 scanning analyses of rsTRPA1 (A-C), bTRPA1 (D-F), and dTRPA1 (G-I) in *Xenopus* oocytes. Upper trace: current recordings at 1 Hz at -60 mV. The extracellular divalent cation conditions are indicated. Middle: temperature change, ~0.5°C/s. The two sets of data points of currents and temperatures producing the maximum Q10 in the recordings are marked with colored circles linked between upper and middle panels. Bottom: Q10 changes throughout the tested temperature range calculated with the interval of 2.5°C. Peak Q10s and Peak Q10-yielding temperatures are indicated. (J) Dot plots of maximum Q10s in the log scale with indicated TRPA1s and extracellular divalent cation conditions. (K) Dot plots of temperatures exhibiting the maximum Q10s (peak temperatures). (L) Dot plots of peak current amplitudes of indicated experiments. **P* < 0.05 and ****P* < 0.001, Tukey's test. #*P* < 0.05, Dunn's test.

(Q10 of 616,595.0) to 2.06 ± 0.27 (Q10 of 114.8) compared with those injected with EGTA that caused a decrement to $\log Q10p$ of 3.64 ± 0.20 (Q10 of 4,365.2). The two chelators are similar in Ca²⁺ affinities at steady state-127 and 149 nM at pH 7.2, respectively (You et al., 1997). The differential effects

of these chelators suggest the fast action of intracellular Ca²⁺ in the potentiation of rsTRPA1 thermosensitivity. This result was recapitulated with 2 mM of external Ba²⁺ (Figs. 2A, 2D-2F), although BAPTA-induced Tp increase was not (Figs. 2B and 2E). We suspected that counteraction of intracellular

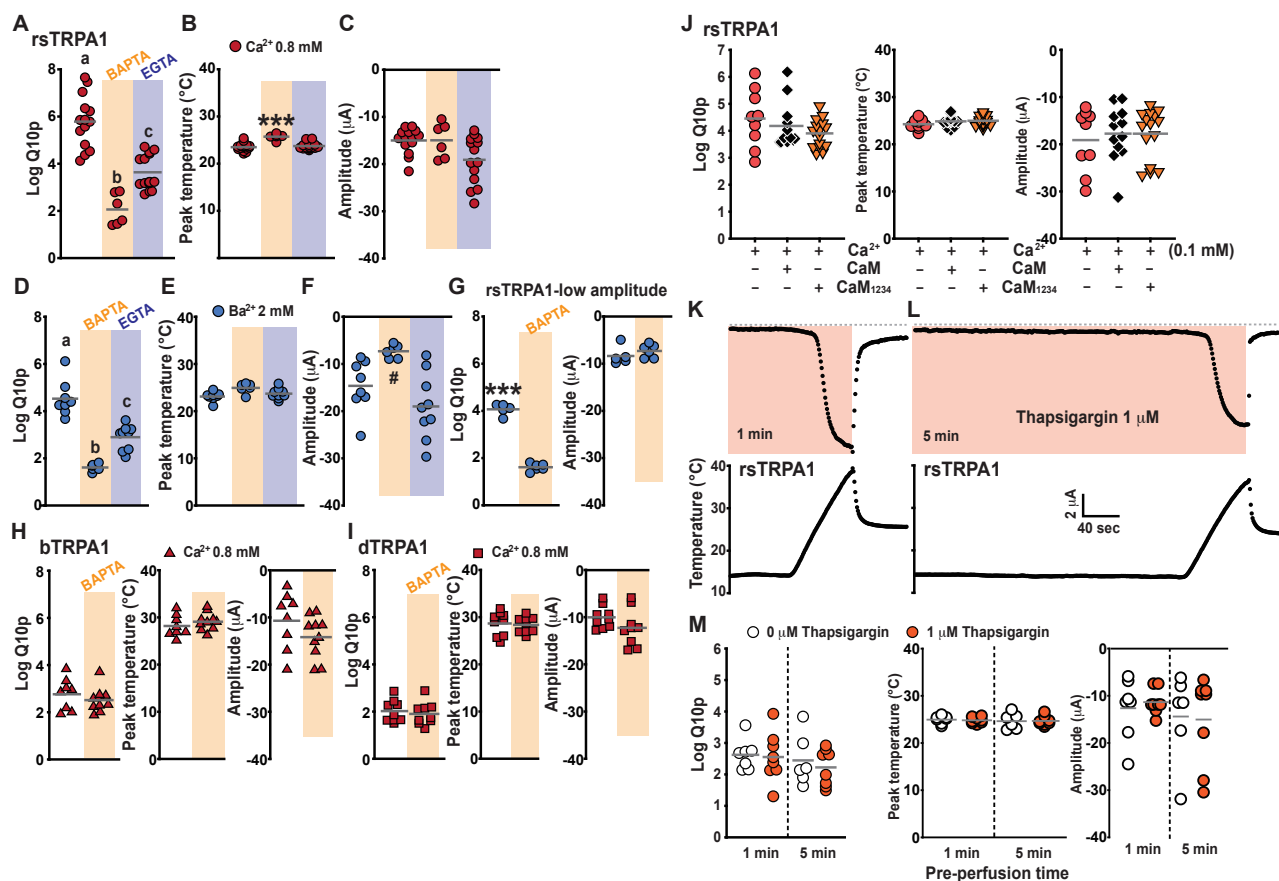


Fig. 2. Intracellular Ca²⁺ chelation suppresses Ca²⁺-dependent hyperthermosensitivity of rattlesnake TRPA1. (A-C) Dot plots of LogQ10ps (A), peak temperatures (B), and current amplitudes (C) of rsTRPA1 with extracellular Ca²⁺ at 0.8 mM. Chelators were microinjected into oocytes to be at 1 and 2.5 mM for BAPTA and EGTA in the cytosol. (D-F) Dot plots of LogQ10ps (D), peak temperatures (E), and current amplitudes (F) of rsTRPA1 with extracellular Ba²⁺ at 0.8 mM indicated conditions. Chelators were microinjected as done in Figs. 2A-2C. (G) Cells with small current amplitudes were compared as BAPTA/Ba²⁺ experiments yielded low amplitudes (F). (H and I) Thermosensitivities and associated parameters of cells expressing bTRPA1 (H) or dTRPA1 (I) were not affected by BAPTA microinjection. (J) Overexpression of calmodulin WT and the CaM₁₂₃₄ mutant did not change rsTRPA1 thermosensitivity. (K-M) Short (K) and long (L) application of 1 μM thapsigargin did not activate rsTRPA1 before temperature ramps or shift its thermosensitivity. Letters indicate statistically distinct groups (Tukey's test): *P* < 0.01 (A), *P* < 0.001 (D). ****P* < 0.001, Tukey's test; #*P* < 0.05, Dunn's test.

BAPTA against Ba²⁺-provoked Q10s of rsTRPA1 may be artifactual because the current amplitudes expressed in the experiment were particularly low (Fig. 2F). Nevertheless, the BAPTA-uninjected and Ba²⁺-perfused control group binned with cells registering current amplitudes similar to those of the BAPTA/Ba²⁺ experiment supported a dramatic drop of Q10s in rsTRPA1-expressing cells by intracellular BAPTA (Fig. 2G). In contrast to rsTRPA1-expressing cells, Q10s of bTRPA1 or dTRPA1-expressing oocytes were little affected by BAPTA injections (Figs. 2H and 2I), indicating bTRPA1 Q10 potentiation only by extracellular Ca²⁺. Interestingly, BAPTA-injected rsTRPA1-expressing oocytes showed Q10s similar to BAPTA-uninjected bTRPA1-expressing cells (Figs. 2A and 2H), implying that intracellular potentiation by permeating Ca²⁺ substantially contributes to the higher thermosensitivity of rsTRPA1 than that of bTRPA1. Unlike mammalian TRPA1s regulated by calmodulin (CaM) (Hasan et al., 2017), rsTRPA1-expressing oocytes showed Q10p values similar to

those concomitantly overexpressing either CaM WT or the CaM₁₂₃₄ mutant (Chang et al., 2018) lacking the Ca²⁺-binding ability (Fig. 2J) in the presence of 0.1 mM extracellular Ca²⁺, suggesting that there is little CaM-dependent potentiation/inhibition of rsTRPA1 thermosensitivity. Also, unlike a previous report on the activation of human TRPA1 (hTRPA1) by thapsigargin-induced Ca²⁺ release (Zurborg et al., 2007), Ca²⁺ from the endoplasmic reticulum (ER) by either a 1 or 5 min application of 1 μM thapsigargin failed to show significant current increases before or shifts in Q10s during temperature ramps (Figs. 2K-2M). The inability of Ca²⁺ from the ER to activate rsTRPA1 or modulate its thermosensitivity proposes that the precise spatiotemporal action of permeating Ca²⁺ is crucial for and probably limited to rsTRPA1 thermosensitivity rather than direct activation.

A previous report (Zurborg et al., 2007) found that a small stretch of the primary sequence in the twelfth N-terminal ankyrin repeat is responsible for Ca²⁺ binding and Ca²⁺-de-

pendent hTRPA1 activation. This EF-hand-like sequence is relatively well conserved in rsTRPA1 and bTRPA1 (Figs. 3A [red line] and 3B). Similarly to hTRPA1, size-conserved substitutions in the domain abolishing negative charges (D476N and D477N) resulted in insensitivity of rsTRPA1 to externally applied Ca²⁺ and Ba²⁺ (Figs. 3E, 3G, and 3I). However, distinctive to hTRPA1, rsTRPA1D485N retained thermosensitivity provoked by the divalent cations (Figs. 3A, 3H, and 3I, Supplementary Fig. S2), as opposed to the corresponding D477A variant of hTRPA1 (Fig. 3A, right gray arrowhead) previously characterized with severe impairment in Ca²⁺-dependent activation (Zurborg et al., 2007). Interestingly, rsTRPA1 with the charge-conservative replacements D476E and D477E did

retain Ca²⁺-dependent, but not Ba²⁺-dependent Q10 boosts (Figs. 3D, 3F, and 3I, Supplementary Fig. S2). The elongated acidic side chains may sterically hinder physical accommodation of Ba²⁺ in the putative binding pocket composed of the EF-hand-like sequence, as Ba²⁺ is larger in diameter than Ca²⁺. Such persistent Ca²⁺-responding capability of rsTRPA1 variants with charge- but not size-conservative changes strongly argues that the conserved EF-hand-like sequences indeed form an intracellular binding structure of divalent cations which critically assists the thermal gating of rsTRPA1.

Intriguingly, sequence comparison between the putative cytosolic Ca²⁺-binding domain of rs- and bTRPA1s reveals a natural variation at D476 in rsTRPA1 to be K475 in bTRPA1,

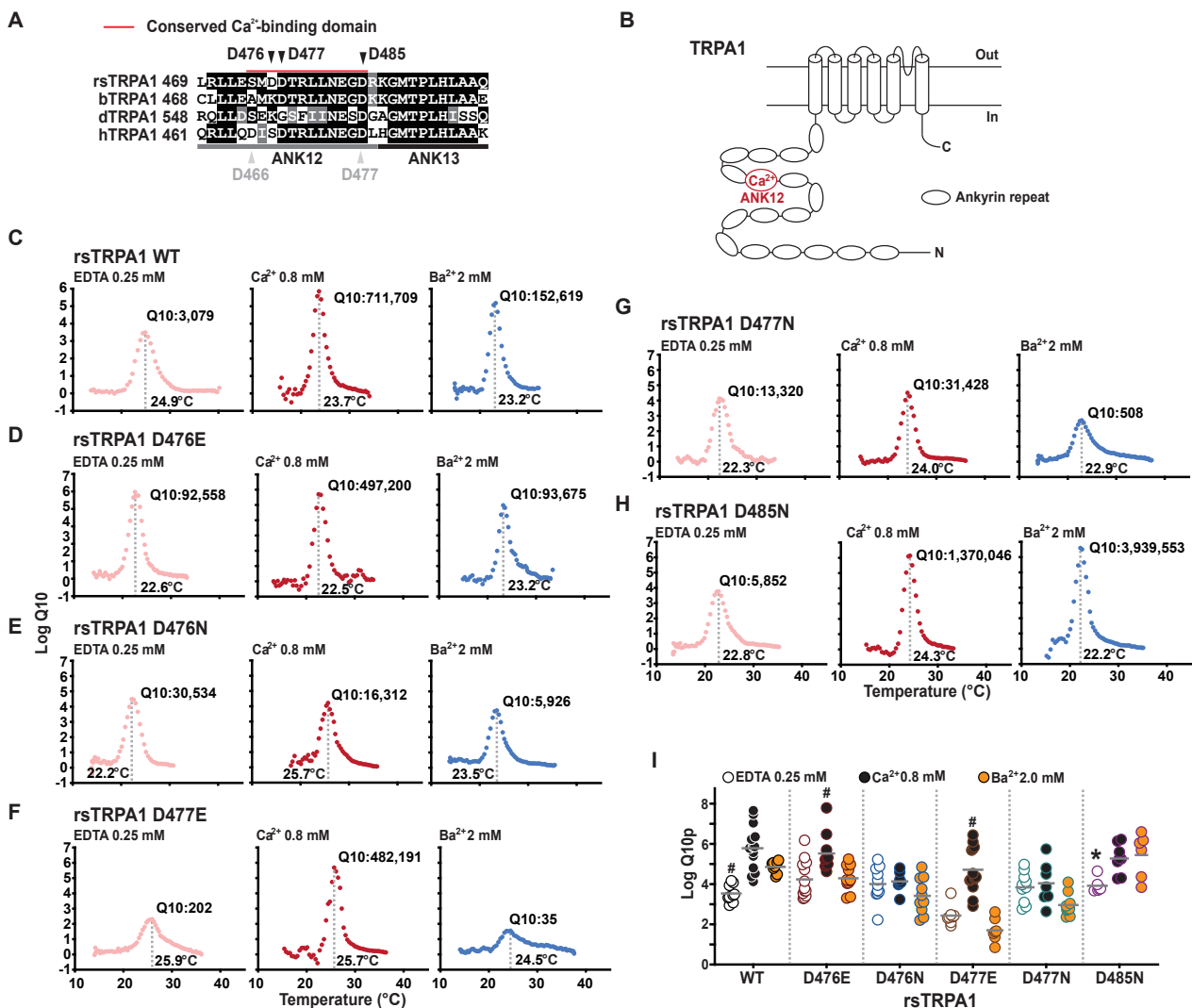


Fig. 3. The conserved cytosolic Ca²⁺-binding domain is required for Ca²⁺-dependent potentiation of rsTRPA1 thermosensitivity. (A) Sequence alignment of the conserved Ca²⁺-binding domain sequence previously identified in human TRPA1 (red line) with those of snake and fruit fly TRPA1s. Gray and black lines mark ankyrin repeats. Gray arrowheads: acidic residues previously characterized to be important for Ca²⁺ binding. Black arrowheads: acidic residues tested in this study. (B) Scheme for location of the conserved Ca²⁺-binding domain in the secondary structure of TRPA1. (C-H) Typical Q10 analyses of rsTRPA1 variants with varying extracellular divalent cation conditions as indicated. Peak Q10s and peak temperatures are presented as numbers. (I) Summary of thermosensitivities exhibited by cells expressing indicated rsTRPA1 variants. *P < 0.05, Tukey's test; #P < 0.05, Dunn's test.

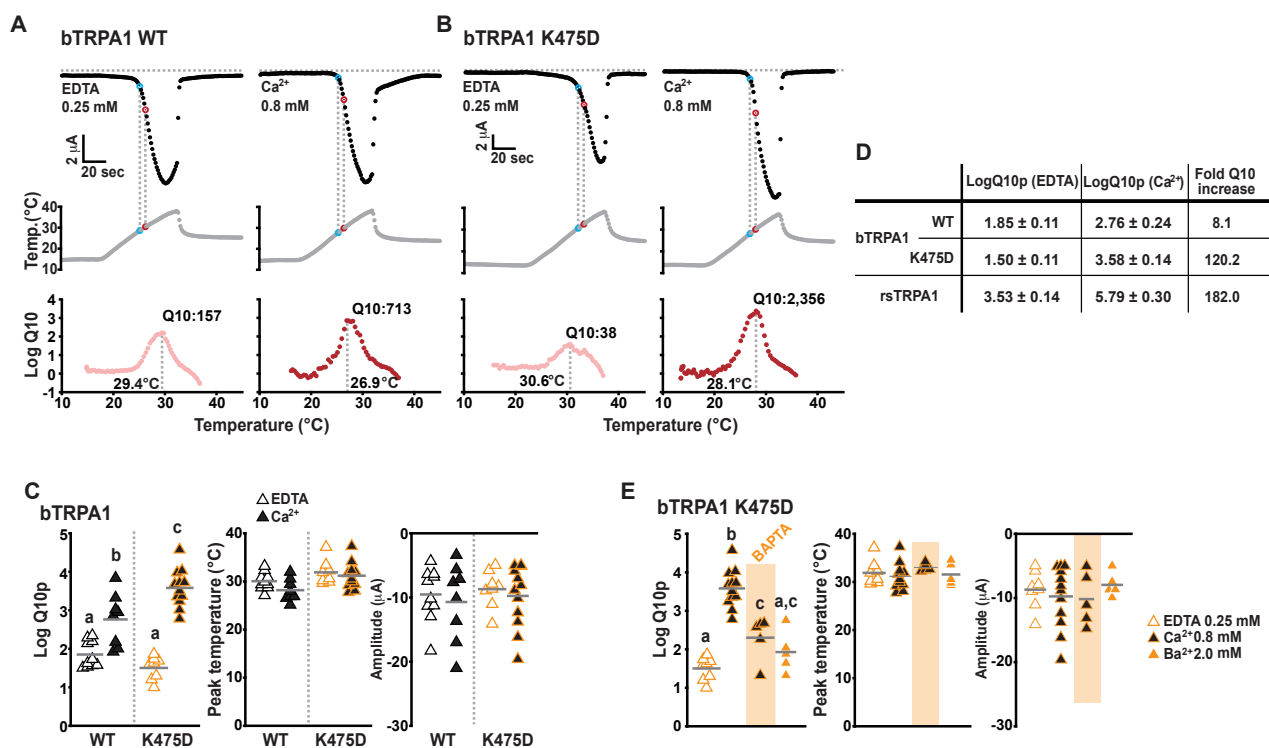


Fig. 4. A rattlesnake-imitating substitution in the putative cytosolic Ca²⁺-binding domain permits bTRPA1 to be potentiated by cytosolic Ca²⁺. (A and B) Representative temperature-sensitive current recording and Q10 scanning of bTRPA1 WT (A) and bTRPA1 K475D (B). (C) Extracellularly applied Ca²⁺ raised thermosensitivity of bTRPA1 K475D higher than that of bTRPA1 WT. (D) Comparison of fold Q10 increases by extracellular Ca²⁺ among bTRPA1s and rsTRPA1. (E) Substantial portion of extracellularly applied Ca²⁺-dependent thermosensitivity is via the cytosol as probed with BAPTA, but unobservable with extracellularly applied Ba²⁺. Letters mark statistically different groups (Tukey's test): *P* < 0.01 (C), *P* < 0.05 (E).

which inverts the charge of a corresponding residue identified above to be functionally important for Ca²⁺-mediated thermosensitivity. If the conserved but putative EF-hand-like sequence of bTRPA1 contains the structural potential accommodating divalent cations, the rattlesnake-imitating substitution K475D may confer bTRPA1 with Ca²⁺- and Ba²⁺-dependent increases of thermosensitivity. Indeed, replacement of the basic with the acidic residue enhanced thermosensitivity of bTRPA1-expressing cells ~6.6 times from WT logQ10p of 2.76 ± 0.24 (Q10 of 575.4) to K475D 3.58 ± 0.14 (Q10 of 3801.9) in the presence of 0.8 mM extracellular Ca²⁺ (Figs. 4A-4D). Furthermore, Q10 of bTRPA1 K475D was improved ~120.2 times by the extracellular addition of 0.8 mM Ca²⁺ compared with extracellularly chelated Ca²⁺ containing 0.25 mM EDTA, while that of bTRPA1 WT was increased only ~8.1 times (Fig. 4D). This result is very interesting in that a single substitution in the dormant cytosolic Ca²⁺-binding domain rendered bTRPA1 to be potentiated by as large a margin as with rsTRPA1; rsTRPA1 thermosensitivity was facilitated ~182.0 times by external 0.8 mM Ca²⁺ compared with the Ca²⁺-chelated condition (Fig. 4D).

Next, by microinjecting BAPTA to a final concentration of 1 mM, we tested whether the dramatic promotion of bTRPA1 thermal responsiveness by the substitution K475D was caused by Ca²⁺ influx as observed above with rsTRPA1. Inter-

estingly, the intracellular BAPTA in cells expressing bTRPA1 K475D accompanied a large reduction of Q10ps albeit in the presence of 0.8 mM extracellular Ca²⁺ (Fig. 4E), bolstering the idea that the majority of acquired Ca²⁺-mediated thermosensitivity stemmed from permeating Ca²⁺. The oocytes in this condition (with little intracellular Ca²⁺ due to BAPTA but 0.8 mM extracellular Ca²⁺), however, had slightly but significantly higher logQ10ps than the oocytes deprived only of extracellular Ca²⁺ (BAPTA-uninjected and perfused in the recording buffer with 0.25 mM EDTA) unlike rsTRPA1 WT (Supplementary Fig. S1B), indicating that the K475D variant retained the ability to be potentiated by extracellular Ca²⁺ as observed with bTRPA1 WT. The K475D replacement did not transform bTRPA1 to be thermally potentiated by Ba²⁺, implying that there are further structural requirements for bTRPA1 to accommodate Ba²⁺ in the conserved cytosolic Ca²⁺-binding domain.

DISCUSSION

Consistent with the thermosensitive model of infrared sense, we previously showed that thermosensitivities of TRPA1s from rattlesnakes and boas can be much higher than molecular thermoreceptors found in non-infrared-sensing animals including *Drosophila* (Kang, 2016a; 2016b). In this study,

we found that thermosensitivities of the snake TRPA1s were upregulated by extracellularly applied Ca²⁺. Interestingly, the mechanisms of Ca²⁺ potentiation in thermal activation were disparate for rsTRPA1 and bTRPA1 in that they require Ca²⁺ at the opposite side of the plasma membrane. The cytosolic Ca²⁺ requirement was endowed by a single substitution in the conserved cytosolic Ca²⁺-binding domain of bTRPA1 (Supplementary Fig. S3A). Such cytosolic Ca²⁺ potentiation of thermal activation may explain the previously reported dramatic Q10/current amplitude relationship observed with rsTRPA1 (Kang, 2016a). Nominally Ca²⁺-free recording solutions without Ca²⁺-buffering reagents such as EDTA are typically used in two-electrode voltage clamping on *Xenopus* oocytes to minimize induction of endogenous CaCC. Nevertheless, free Ca²⁺ ions are often present in the recording solution due to contamination from various sources such as glassware and other chemicals. The physiologically low and thus unsaturating concentrations of Ca²⁺ contamination may then cause rsTRPA1-expressing cells to yield more robust Q10 via cytosolic potentiation of rsTRPA1, when thermosensitive currents through rsTRPA1 are larger to provide higher numbers of permeating Ca²⁺ ions. Thus, the steeply proportional Q10/current amplitude relationships previously obtained with rsTRPA1-expressing cells likely result from permeating-Ca²⁺-mediated potentiation of thermal activation.

One interesting aspect of our results is that cytosolic potentiation by Ca²⁺ correlates with superior thermosensitivities as observed with rsTRPA1 and bTRPA1 K475D: for example, mean Q10ps of ~600,000 and ~575 for intracellularly regulated rsTRPA1 and extracellularly modulated bTRPA1 WT, respectively, and mean Q10ps of ~3,800 and ~575 for intracellularly potentiated bTRPA1 K475D and extracellularly modulated bTRPA1 WT, respectively. This finding suggests that cytosolic potentiation is more effective in promoting thermal activation of TRPA1s than extracellular regulation. A possible explanation for this observation is that the cytosolic Ca²⁺-binding domain may be closely linked with the temperature-sensing domain, so that the two positively regulating pathways intimately work together with synergistic cooperation. Systematic structural mapping, previously conducted by thermally examining various chimeras between rsTRPA1 and hTRPA1 with and without warmth sensitivity, respectively, indeed attributed the capability of thermal activation to two major areas of N-terminal ankyrin repeat domains (Cordero-Morales et al., 2011). Therefore, it is very likely that Ca²⁺ binding to the cytosolic domain greatly affects thermal sensitivity of these domains, as the ankyrin repeat 12 responsible for the cytosolic Ca²⁺ binding in rsTRPA1 is strategically positioned to be a part of or in proximity to the rsTRPA1 domains conferring hTRPA1 with thermal sensitivity. By contrast, chimeric investigation between dTRPA1 and hTRPA1 reported the extracellular pore region as the key area essential for thermal sensitivity (Wang et al., 2013). These inconsistent outcomes may be because of different TRPA1s used in the studies, implying that several areas of the TRPA1 structure operate together to execute the temperature-sensing function, and/or that d- and rsTRPA1 may have divergently evolved to harbor distinct temperature-sensing mechanisms for the sensation of warmth.

Acquisition of cytosolic Ca²⁺ sensitivity by a single substitution in bTRPA1 suggests that the loss of cytosolic Ca²⁺-mediated potentiation may be a recent evolutionary event in boas, as bTRPA1 retains other structural features required for the Ca²⁺-mediated potentiation. Supporting this possibility, sequence alignments show that the amino acid residue corresponding to K475 in bTRPA1 is mostly conserved with an acid residue in a wide range of snake species as well as *Eryx tataricus*, another species in the boidae (Supplementary Fig. S3B). However, because TRPA1s from pythons, another group of pit-bearing snakes considered to be ancient like boas (Gracheva et al., 2010), have single prolines in this site with charge-neutralizing characteristics similar to our rsTRPA1 D476N mutant and thus supposedly removing intracellular Ca²⁺ binding, it cannot be excluded that other snake TRPA1s have recently acquired the acidic residue for cytosolic potentiation. Further functional and systemic investigations with TRPA1s from various snake species will be necessary for a clear picture on the molecular evolution of cytosolic Ca²⁺-mediated potentiation in snake TRPA1s. It is also interesting to discover the evolutionary driving force for the wide adaptation of cytosolic Ca²⁺-mediated potentiation to the snakes unrelated to infrared senses. Conversely, if TRPA1s from infrared-sensing boa and pythons have recently lost cytosolic potentiation by Ca²⁺, there must have been an environmental pressure against hyper-thermosensitivity of the TRPA1s, of which ecological significances would be a subject of interest.

Contribution of permeating Ca²⁺ to channel modulation has been known for many sensory functions of TRP channels (Hasan and Zhang, 2018). Mammalian TRPA1s require cytosolic Ca²⁺ to be robustly activated by hydrogen peroxide (Andersson et al., 2008) and cold temperatures (Zurborg et al., 2007) as well as to be negatively regulated (Wang et al., 2008), while Ca²⁺ alone can trigger channel activation (Zurborg et al., 2007). Similarly, activation of TRPM8 by icilin needs to coincide with intracellular Ca²⁺ induced by either channel permeation or release from the intracellular Ca²⁺ storage (Chuang et al., 2004). In the case of rsTRPA1, Ca²⁺ only serves as a positive regulator rather than a requirement for thermal activation, which may widen the dynamic range of thermosensitivity that rsTRPA1 can exhibit. As cytosolic potentiation by permeating Ca²⁺ is an intrinsic property of rsTRPA1 embedded by the simple conserved sequence stretch as observed here and necessarily associated with the opening of Ca²⁺-conducting rsTRPA1 in physiological conditions, our findings in the heterologous expression system likely have relevance to *in vivo* settings in the rattlesnake pit membrane.

Note: Supplementary information is available on the Molecules and Cells website (www.molcells.org).

ACKNOWLEDGMENTS

This work was supported by the National Research Foundation of Korea (NRF-2015R1D1A1A01057288, NRF-2017R1A4A1015534, NRF-2018R1A2B6003321 to K.K. and 2020R111A1A01071613 to E.J.D.) funded by the Korean Government (Ministry of Education and Ministry of Science, ICP and Future Planning).

AUTHOR CONTRIBUTIONS

K.K. and E.J.D. designed experiments, analyzed data, and wrote the paper, E.J.D. performed oocyte physiology.

CONFLICT OF INTEREST

The authors have no potential conflicts of interest to disclose.

ORCID

Eun Jo Du <https://orcid.org/0000-0002-5600-724X>
KyeongJin Kang <https://orcid.org/0000-0003-0446-469X>

REFERENCES

- Andersson, D.A., Gentry, C., Moss, S., and Bevan, S. (2008). Transient receptor potential A1 is a sensory receptor for multiple products of oxidative stress. *J. Neurosci.* *28*, 2485-2494.
- Bakken, G.S. and Krochmal, A.R. (2007). The imaging properties and sensitivity of the facial pits of pitvipers as determined by optical and heat-transfer analysis. *J. Exp. Biol.* *210* (Pt 16), 2801-2810.
- Bullock, T.H. and Fox, W. (1957). The anatomy of the infra-red sense organ in the facial pit of pit vipers. *J. Cell Sci.* *98*, 219-234.
- Campbell, A.L., Naik, R.R., Sowards, L., and Stone, M.O. (2002). Biological infrared imaging and sensing. *Micron* *33*, 211-225.
- Chang, A., Abderemane-Ali, F., Hura, G.L., Rossen, N.D., Gate, R.E., and Minor, D.L., Jr. (2018). A calmodulin C-lobe Ca²⁺-dependent switch governs Kv7 channel function. *Neuron* *97*, 836-852.e6.
- Chuang, H.H., Neuhauser, W.M., and Julius, D. (2004). The super-cooling agent icilin reveals a mechanism of coincidence detection by a temperature-sensitive TRP channel. *Neuron* *43*, 859-869.
- Clapham, D.E. and Miller, C. (2011). A thermodynamic framework for understanding temperature sensing by transient receptor potential (TRP) channels. *Proc. Natl. Acad. Sci. U. S. A.* *108*, 19492-19497.
- Cordero-Morales, J.F., Gracheva, E.O., and Julius, D. (2011). Cytoplasmic ankyrin repeats of transient receptor potential A1 (TRPA1) dictate sensitivity to thermal and chemical stimuli. *Proc. Natl. Acad. Sci. U. S. A.* *108*, E1184-E1191.
- de Cock Buning, T. (1983). Thresholds of infrared sensitive tectal neurons in *Python reticulatus*, *Boa constrictor* and *Agkistrodon rhodostoma*. *J. Comp. Physiol.* *151*, 461-467.
- Du, E.J., Ahn, T.J., Kwon, I., Lee, J.H., Park, J.H., Park, S.H., Kang, T.M., Cho, H., Kim, T.J., Kim, H.W., et al. (2016a). TrpA1 regulates defecation of food-borne pathogens under the control of the Duox pathway. *PLoS Genet.* *12*, e1005773.
- Du, E.J., Ahn, T.J., Sung, H., Jo, H., Kim, H.W., Kim, S.T., and Kang, K. (2019). Analysis of phototoxin taste closely correlates nucleophilicity to type 1 phototoxicity. *Proc. Natl. Acad. Sci. U. S. A.* *116*, 12013-12018.
- Du, E.J., Ahn, T.J., Wen, X., Seo, D.W., Na, D.L., Kwon, J.Y., Choi, M., Kim, H.W., Cho, H., and Kang, K. (2016b). Nucleophile sensitivity of *Drosophila* TRPA1 underlies light-induced feeding deterrence. *Elife* *5*, e18425.
- Gracheva, E.O., Ingolia, N.T., Kelly, Y.M., Cordero-Morales, J.F., Hollopeter, G., Chesler, A.T., Sánchez, E.E., Perez, J.C., Weissman, J.S., and Julius, D. (2010). Molecular basis of infrared detection by snakes. *Nature* *464*, 1006-1011.
- Guinamard, R., Simard, C., and Del Negro, C. (2013). Flufenamic acid as an ion channel modulator. *Pharmacol. Ther.* *138*, 272-284.
- Hamada, F.N., Rosenzweig, M., Kang, K., Pulver, S.R., Ghezzi, A., Jegla, T.J., and Garrity, P.A. (2008). An internal thermal sensor controlling temperature preference in *Drosophila*. *Nature* *454*, 217-220.
- Hasan, R., Leeson-Payne, A.T., Jaggar, J.H., and Zhang, X. (2017). Calmodulin is responsible for Ca²⁺-dependent regulation of TRPA1 channels. *Sci. Rep.* *7*, 45098.
- Hasan, R., and Zhang, X. (2018). Ca²⁺ regulation of TRP ion channels. *Int. J. Mol. Sci.* *19*, E1256.
- Kang, K. (2016a). Exceptionally high thermal sensitivity of rattlesnake TRPA1 correlates with peak current amplitude. *Biochim. Biophys. Acta* *1858*, 318-325.
- Kang, K. (2016b). Thermal sensitivity analysis data utilizing Q10 scanning, Boltzmann slope factor and the change of molar heat capacity. *Data Brief* *6*, 732-737.
- Kang, K., Panzano, V.C., Chang, E.C., Ni, L., Dainis, A.M., Jenkins, A.M., Regna, K., Muskavitch, M.A., and Garrity, P.A. (2012). Modulation of TRPA1 thermal sensitivity enables sensory discrimination in *Drosophila*. *Nature* *481*, 76-80.
- Kang, K., Pulver, S.R., Panzano, V.C., Chang, E.C., Griffith, L.C., Theobald, D.L., and Garrity, P.A. (2010). Analysis of *Drosophila* TRPA1 reveals an ancient origin for human chemical nociception. *Nature* *464*, 597-600.
- Kang, K.J., Kinjo, T.G., Szerencsei, R.T., and Schnetkamp, P.P. (2005a). Residues contributing to the Ca²⁺ and K⁺ binding pocket of the NCKX2 Na⁺/Ca²⁺-K⁺ exchanger. *J. Biol. Chem.* *280*, 6823-6833.
- Kang, K.J., Shibukawa, Y., Szerencsei, R.T., and Schnetkamp, P.P. (2005b). Substitution of a single residue, Asp575, renders the NCKX2 K⁺-dependent Na⁺/Ca²⁺ exchanger independent of K⁺. *J. Biol. Chem.* *280*, 6834-6839.
- Liu, B., Hui, K., and Qin, F. (2003). Thermodynamics of heat activation of single capsaicin ion channels VR1. *Biophys. J.* *85*, 2988-3006.
- Noble, G.K. and Schmidt, A. (1937). The structure and function of the facial and labial pits of snakes. *Proc. Am. Philos. Soc.* *77*, 263-288.
- Oh, S.J., Hwang, S.J., Jung, J., Yu, K., Kim, J., Choi, J.Y., Hartzell, H.C., Roh, E.J., and Lee, C.J. (2013). MONNA, a potent and selective blocker for transmembrane protein with unknown function 16/anoctamin-1. *Mol. Pharmacol.* *84*, 726-735.
- Oh, S.J., Park, J.H., Han, S., Lee, J.K., Roh, E.J., and Lee, C.J. (2008). Development of selective blockers for Ca²⁺-activated Cl channel using *Xenopus laevis* oocytes with an improved drug screening strategy. *Mol. Brain* *1*, 14.
- Wang, H., Schupp, M., Zurborg, S., and Heppenstall, P.A. (2013). Residues in the pore region of *Drosophila* transient receptor potential A1 dictate sensitivity to thermal stimuli. *J. Physiol.* *591*, 185-201.
- Wang, Y.Y., Chang, R.B., Waters, H.N., McKemy, D.D., and Liman, E.R. (2008). The nociceptor ion channel TRPA1 is potentiated and inactivated by permeating calcium ions. *J. Biol. Chem.* *283*, 32691-32703.
- Warren, J.W. and Proske, U. (1968). Infrared receptors in the facial pits of the Australian python *Morelia spilotes*. *Science* *159*, 439-441.
- You, Y., Pelzer, D.J., and Pelzer, S. (1997). Modulation of L-type Ca²⁺ current by fast and slow Ca²⁺ buffering in guinea pig ventricular cardiomyocytes. *Biophys. J.* *72*, 175-187.
- Zurborg, S., Yurgionas, B., Jira, J.A., Caspani, O., and Heppenstall, P.A. (2007). Direct activation of the ion channel TRPA1 by Ca²⁺. *Nat. Neurosci.* *10*, 277-279.